Numerical Analysis of Non-Fourier Heat Transfer in a Solid Cylinder with Dual-Phase-Lag Phenomenon

M. H. Ghasemi[1], S. Hoseinzadeh[2, 3, *], P. S. Heyns[2] and D. N. Wilke[2]

Abstract: In this study, transient non-Fourier heat transfer in a solid cylinder is analytically solved based on dual-phase-lag for constant axial heat flux condition. Governing equations for the model are expressed in two-dimensional cylindrical coordinates; the equations are nondimensionalized and exact solution for the equations is presented by using the separation of variable method. Results showed that the dual-phase-lag model requires less time to meet the steady temperature compared with single-phase-lag model. On the contrary, thermal wave diffusion speed for the dual-phase-lag model is greater than the single-phase-lag model. Also the effect of relaxation time in dual-phase-lag model has been taken on consideration.

Keywords: Exact solution, non-Fourier heat transfer, dual-phase-lag, cylindrical coordinate.

1 Introduction

In classical Fourier heat transfer equation, heat flux has a direct relationship with temperature gradient and, accordingly, these occur simultaneously. Therefore, the heat wave is propagated with infinite rate; in cases where heat flux or temperature gradient changes rapidly, the results of Fourier equation are not consistent with experimental results. Fourier's law is not adequately precise for analyzing cases such as rapid high frequency heating such as laser and microwave, low temperature conditions near absolute zero, application of non-homogeneous materials such as sand and glass, and examination of materials with a slow thermal response time structure, such as biological tissues. Maurer et al. [Maurer and Thompson (1973)] according to empirical observations concluded that when heat flux is above 10^7 watts/cm² with time scale of less than 150 PS, Fourier heat flux model, which is called classical theory, is rejected.

Cattaneo [Cattaneo (1958)] and Vernote [Vernote (1958)] separately provided an equation for conductivity heat transfer, called the telegraph equation in solids or C-V Model with the introduction of a time lag in the appearance of heat flux.

---

[1] Department of Mechanical Engineering, West Tehran Branch, Islamic Azad University, Tehran, Iran.

[2] Centre for Asset Integrity Management, Department of Mechanical and Aeronautical Engineering, University of Pretoria, Pretoria, South Africa.

[3] Young Researchers and Elite Club, West Tehran Branch, Islamic Azad University, Tehran, Iran.

[*] Corresponding Author: Siamak Hoseinzadeh. Email: Hoseinzadeh.siamak@gmail.com;
  Hosseinzadeh.siamak@up.ac.za.

Tizo [Tizo (1992)] presented the general equation of C-V model, called single-phase lag model; Based on single-phase lag equation, the temperature gradient created at place r and time t caused heat flux at place r and the next time $t + \tau_q$, where τ_q is inertia time or lag time that shows the time required to collect energy to transfer heat between structural elements. The lag time with the first order approximation of Taylor expansion of heat flux in the single-phase lag equation becomes the C-V equation.

For many solids, inertia time is in the range of 10^{-10} to 10^{-14} seconds and for gases is in the range of 10^{-8} to 10^{-10} seconds. Of course, this range increases for some biological materials and some materials with a non-homogeneous structure by 10^2 [Wang, Zhou and Wei (2008)].

Although many researchers have used the C-V equation widely in applications such as low temperatures [Cimmelli and Frischmuth (1996)], materials with a non-homogeneous internal structure [Antaki (2005)], high heat flux, laser short-pulse heating [Qiu and Tien (1993)] and heating of materials with micro and nano structures [Tzou (2014)], C-V model is contrary to Clausius's theorem. Because C-V wave model may yield results in positive and negative values of entropy generation rate, which, in analyzing the second law, is incompatible with local thermodynamics equilibrium theory [Askarizadeh and Baniasadi (2017)].

The research showed that C-V equation ignored microstructure interactions in small-scale heat transfer only by taking into account the rapid transfer effects. Thus, Tizo [Tizo (1995)] provided the improved model of dual time lag called dual phase lag; Tizo introduced two inherent thermal properties of the system (τ_T and τ_q); The lag time τ_T is called fuzzy lag of temperature gradient and indicates the effect of small spatial scales on heat transfer. In other words, τ_q represents thermal inertia and τ_T represents microstructures' response.

Talaee et al. [Talaee and Atefi (2011)] examined non-Fourier conductivity heat transfer equation with C-V model in a hollow cylinder with alternating flux and provided an analytical solution. In the study, they considered the homogeneous and isotropic cylinder. In the study, the results for time independent heat flux were obtained variables' separation method and the results of time-dependent heat flux are obtained from two-factor integral.

Saedodin et al. [Saedodin and Barforoush (2012, 2017)] investigated non-Fourier heat transfer equation with C-V model in a solid cylinder with constant heat flux. They used variables' separation method for solving their non-Fourier heat transfer equation and the effect of increasing V Number on temperature profile.

Talaee et al. [Talaee, Sarafrazi and Bakhshandeh (2016)] in their study solved the C-V heat transfer equation in a cube by applying pulsed heat flux. In this study, the exact solution presented was based on variables' separation method and two-factor integral. The study results showed that a significant difference was found between the profiles of Fourier and non-Fourier temperature.

Fu et al. [Fu, Chen, Qian et al. (2014)] examined the effect of a sudden change in the temperature of a gap at the outer surface of a solid cylinder. They considered non-Fourier heat transfer equation according to C-V model and used Laplace transform method to solve it.

Liu et al. [Liu and Chang (2007)] investigated non-Fourier conductivity heat transfer of dual-phase lag in a solid cylinder with regressive exponential pulsed variable heat flux. In order to solve the problem, they simultaneously applied Laplace transform method and

control volume theory to solve their equations. And the effects of time lag rate, time shift, and shape of pulsed heat function have been studied on heat transfer behavior.

Wu et al. [Wu, Lee, Chang et al. (2015)] in order to solve hyperbolic heat conductivity inverse problem used dual phase lag heat transfer model to estimate pulsed heat flux in an infinite solid cylinder. They performed their analysis based on numerical methods of Laplace transform and volume control.

Julius et al. [Julius, Lizronock and Socorel (2018)] conducted a comprehensive study on a one-dimensional non-Fourier heat transfer with a dual phase lag model on a single sheet. They have solved their equations by integrating the analytical method and considering time-dependent heat production and combining different boundary conditions (Dirichlet, Newman and Robin).

Wang et al. [Wang, Xu and Zhou (2001)] used separation of the variables method to solve C-V and dual-phase-lagging heat conduction equations in a finite 1D region under Dirichlet, Neumann or Robin boundary conditions, stability of solution in initial condition was considered.

Non-Fourier heat conduction problem in finite rigid slabs effected by short pulse lasers analytically was solved by using Green's functions and the finite integral transform technique [Tang and Araki (1999); Abdel-Hamid (1999)].

Moosaie et al. [Moosaie, Atefi and Fardad (2008)] analytically solved hyperbolic heat conduction equation under arbitrary initial condition for rectangular plate with homogeneous boundary conditions of first type; Temperature field was a double Fourier series and the solution was valid even for discontinuous but integrable initial conditions. Also Moosaie [Moosaie (2008)] investigated axisymmetric temperature field in a hollow sphere by using C-V hyperbolic heat conduction equation and separation of variables method to solve the problem.

Analytical solution of hyperbolic heat equation in a hollow sphere under pulse lasers was obtained by Shirmohammadi [Shirmohammadi (2008)]. The temperature distribution, the propagation and reflection of the temperature wave due to such heat pulse was investigated or different thermal relaxation times and laser pulse duration.

Nonlinear heat transfer in a fin problem with presuming the thermal conductivity is a linear function of temperature and the heat transfer coefficient is expressed in a power-law form was considered by Anbarloei et al. [Anbarloei and Shivanian. (2016)].

Tsai et al. [Tsai and Hung (2003)] considered Thermal behavior of a solid and a hollow sphere due to a sudden temperature change on the outer surface by Laplace transformation and the Riemann-sum approximation. Effects of the relaxation time, the imposed temperature ratio on the inner and outer layers of the hollow sphere, the thermal diffusivity ratio, and the relaxation time ratio of the composite sphere were studied [Tsai, lin and Hung (2005)].

Jiang [Jiang (2006)] solved The hyperbolic heat equation process in a hollow sphere with boundary surfaces subject to sudden temperature change by analytically means of integration transformation. An analytically solution of hyperbolic equation in a hollow sphere under harmonic boundary condition was considered by Bahrami et al. [Bahrami, Hosseinzadeh, Ghasemiasl et al. (2015)]. Methods of solution of this work were the standard separation of variables method and Duhamel integral for applying the time-dependent boundary conditions.

Babaei et al. [Babaei and Chen (2008)] investigated Non Fourier Hyperbolic heat conduction in a heterogeneous sphere. All material properties except relaxation time were assumed vary continuously within the sphere in the radial direction following a power law and the solution was obtained by using numerical inversion of the Laplace transform.

Unsteady conductive heat transfer in multilayer spherical composite laminates under linear boundary conditions consisting of the conduction, convection, and radiation heat transfer is considered analytically by Amiri et al. [Amiri and Norouzi (2015)]. Laplace transform and separation of variables were utilized to obtain exact solution.

Askarizadeh et al. [Askarizadeh and Ahmadikia (2018)] studied a high-order dual-phase-lag (DPL) heat transfer equation and its thermodynamic consistency. Compatibility of first and second-order approximations of the DPL model with the traditional second law of thermodynamics was shown in the analytical approach.

Xu [Xu (2011)] considered the paradox of the thermal vibration phenomenon occurring in the dual-phase-lagging heat conduction with second law of thermodynamics. He developed two types of the extended irreversible thermodynamics to fix this paradox.

In this study, the exact solution of the heat transfer equation in a solid cylinder with special constant heat flux in a part of the cylinder axis based on the dual phase lag model is investigated using variables' separation method. It can cover a wide range of issues, such as: resizing the heat flux boundary with time, heat flux acting boundary function, and the effect of constant flux applied displacement.

2 Problem statement

In the present study, heat transfer equation of a solid cylinder with a dual phase lag model is considered in accordance with Fig. 1.
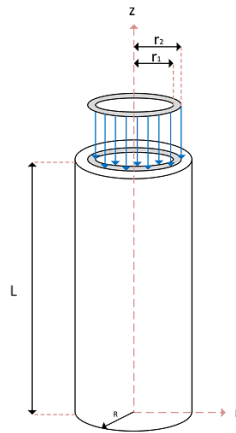

Figure 1: A cylinder with axial heat flux

Assuming that the object is homogeneous and isotropic, the governing equations for heat transfer are expressed for temperature field $T(r.z.t)$ as follow:

$$\alpha \left(\frac{\partial T}{\partial t} + \tau_q \frac{\partial^2 T}{\partial t^2} \right) = \frac{\partial^2 T}{\partial r^2} + \frac{1}{r}\frac{\partial T}{\partial r} + \frac{\partial^2 T}{\partial z^2} + \tau_T \frac{\partial}{\partial t}\left(\frac{\partial^2 T}{\partial r^2} + \frac{1}{r}\frac{\partial T}{\partial r} + \frac{\partial^2 T}{\partial z^2} \right) \tag{1}$$

where α is the thermal diffusivity coefficient and τ_T and τ_q are the phase lag of the temperature gradient and heat flux, respectively.

The boundary conditions of the problem are assumed as follow:

$$\frac{\partial T(0.z.t)}{\partial r} = 0 \tag{2-a}$$

$$T(R.z.t) = T_\infty \tag{2-b}$$

$$T(r.0.t) = T_\infty \tag{2-c}$$

$$K\frac{\partial T(r.L.t)}{\partial z} = \begin{cases} 0 & r < r_1 \\ q & r_1 < r < r_2 \\ 0 & r > r_2 \end{cases} \tag{2-d}$$

The Initial conditions are considered as follows:

$$T(r.z.0) = T_\infty \tag{3-a}$$

$$\frac{\partial T}{\partial t}(r.z.0) = 0 \tag{3-b}$$

3 Method of solution

In order to compare and analyze the data, dimensionless parameters are defined as follow:

$$\xi = \frac{r}{R}; \qquad Fo = \frac{\alpha_0 t}{L^2}; \qquad \theta = K\frac{T-T_\infty}{Lq_0}; \qquad \alpha_0 = \frac{K_0}{\rho_0 c_0}; \tag{4}$$

$$\omega = \frac{z}{L}; \quad Ve_T = \sqrt{\frac{\alpha_0 \tau_T}{L^2}}; \qquad Ve_q = \sqrt{\frac{\alpha_0 \tau_q}{L^2}}; \quad M = \frac{L}{R} \tag{5}$$

The dimensionless parameters are applied to heat transfer equations and boundary and primary conditions. In this way, heat transfer equation with dual phase lag is obtained as follows:

$$\left(\frac{\partial\theta}{\partial Fo} + Ve_q{}^2\frac{\partial^2\theta}{\partial Fo^2}\right) = M^2\frac{\partial^2\theta}{\partial\xi^2} + \frac{M^2}{\xi}\frac{\partial\theta}{\partial\xi} + \frac{\partial^2\theta}{\partial\omega^2} + Ve_T{}^2\frac{\partial}{\partial Fo}\left(M^2\frac{\partial^2\theta}{\partial\xi^2} + \frac{M^2}{\xi}\frac{\partial\theta}{\partial\xi} + \frac{\partial^2\theta}{\partial\omega^2}\right) \tag{6}$$

And boundary dimensionless conditions are equal to

$$\frac{\partial\theta(0.\omega.Fo)}{\partial\xi} = 0 \tag{7-a}$$

$$\theta(1.\omega.Fo) = 0 \tag{7-b}$$

$$\theta(\xi.0.Fo) = 0 \tag{7-c}$$

$$\frac{\partial\theta(\xi.1.Fo)}{\partial\omega} = \begin{cases} 0 & \xi < \xi_1 \\ 1 & \xi_1 < \xi < \xi_2 \\ 0 & \xi > \xi_2 \end{cases} \tag{7-d}$$

And dimensionless initial conditions are rewritten as follow:

$$\theta(\xi.\omega.0) = 0 \tag{8-a}$$

$$\frac{\partial\theta}{\partial Fo}(\xi.\omega.0) = 0 \tag{8-b}$$

Özisik [Özisik (2013)] divided the solution of Eq. (6) into total of steady and unsteady problems as follows:

$$\theta(\xi.\omega.Fo) = \psi(\xi.\omega.Fo) + \phi(\xi.\omega) \tag{9}$$

That φ (ξ.ω) is a steady problem solution with heterogeneous boundary conditions and ψ

($\xi.\omega.Fo$) is a transient problem solving with homogeneous boundary conditions.

3.1 Steady problem

The equation of the steady state is obtained as follows:

$$M^2 \frac{\partial^2 \phi}{\partial \xi^2} + \frac{M^2}{\xi} \frac{\partial \phi}{\partial \xi} + \frac{\partial^2 \phi}{\partial \omega^2} = 0 \tag{10}$$

And the boundary conditions of the problem are as follows:

$$\frac{\partial \phi(0.\omega)}{\partial \xi} = 0 \tag{11-a}$$

$$\phi(1.\omega) = 0 \tag{11-b}$$

$$\phi(\xi.0) = 0 \tag{11-c}$$

$$\frac{\partial \phi(\xi.1)}{\partial \omega} = \begin{cases} 0 & \xi < \xi_1 \\ 1 & \xi_1 < \xi < \xi_2 \\ 0 & \xi > \xi_2 \end{cases} \tag{11-d}$$

Eq. (10) can be written using variables' separation method as follows:

$$\phi(\xi.\omega) = X(\xi)Z(\omega) \tag{12}$$

With applying Eq. (12) to Eq. (10), Eq. (13) is obtained as follows:

$$\frac{M^2}{X}\left(\frac{\partial^2 X}{\partial \xi^2} + \frac{1}{\xi}\frac{\partial X}{\partial \xi}\right) = -\frac{1}{Z}\frac{\partial^2 Z}{\partial \omega^2} = -\gamma^2 \tag{13}$$

Eq. (13) is divided into two distinct equations in terms of the variables ξ and ω that the separated equation in the direction of ξ with its boundary conditions is equal to

$$\xi^2 \frac{\partial^2 X}{\partial \xi^2} + \xi \frac{\partial X}{\partial \xi} + \xi^2 \frac{\gamma^2}{M^2} X = 0 \tag{14}$$

$$B.c \begin{cases} \frac{\partial X(0)}{\partial \xi} = 0 \\ X(1) = 0 \end{cases} \tag{15}$$

The corresponding answer to Eq. (14) is equal to

$$X(\xi) = C_1 J_0\left(\frac{\gamma}{M}\xi\right) + C_2 Y_0\left(\frac{\gamma}{M}\xi\right) \tag{16}$$

With applying the boundary condition Eq. (15), $C_2 = 0$, and Eq. (16) is reduced as follow:

$$X(\xi) = C_1 J_0\left(\frac{\gamma}{M}\xi\right) \tag{17}$$

In Eq. (17), $\frac{\gamma}{M}$ is the solution of the equation $J_0\left(\frac{\gamma}{M}\right) = 0$.

The separated equation in the direction ω and its corresponding boundary conditions are observed in Eqs. (18) and (19)

$$\frac{\partial^2 Z}{\partial \omega^2} - \gamma^2 Z = 0 \tag{18}$$

$$B.c \quad Z(0) = 0 \tag{19}$$

The answer of the differential Eq. (18) is obtained with applying boundary conditions Eq. (19) as follows:

$$Z(\omega) = C sinh(\gamma \omega) \tag{20}$$

The general answer of the steady state Eq. (10) is obtained using variables' separation method as follow:

$$\phi(\xi.\omega) = \sum_{n=1}^{\infty} a_n \, sinh(\gamma_n \omega) J_0\left(\frac{\gamma_n}{M}\xi\right) \tag{21}$$

Using the orthogonal function and boundary conditions Eq. (11-d), a_n is obtained as follow:

$$a_n = \frac{2M\left(-\xi_1 J_1\left(\frac{\gamma_n}{M}\xi_1\right)+\xi_2 J_1\left(\frac{\gamma_n}{M}\xi_2\right)\right)}{\gamma_n^2 \cosh \gamma_n \left[J_1\left(\frac{\gamma_n}{M}\right)\right]^2} \tag{22}$$

3.2 Transient problem

$$\left(\frac{\partial \psi}{\partial Fo} + Ve_q^2 \frac{\partial^2 \psi}{\partial Fo^2}\right) = M^2 \frac{\partial^2 \psi}{\partial \xi^2} + \frac{M^2}{\xi}\frac{\partial \psi}{\partial \xi} + \frac{\partial^2 \psi}{\partial \omega^2} + Ve_T^2 \frac{\partial}{\partial Fo}\left(M^2 \frac{\partial^2 \psi}{\partial \xi^2} + \frac{M^2}{\xi}\frac{\partial \psi}{\partial \xi} + \frac{\partial^2 \psi}{\partial \omega^2}\right) \tag{23}$$

The boundary conditions of the transient problem are equal to:

$$\frac{\partial \psi(0.\omega.Fo)}{\partial \xi} = 0 \tag{24-a}$$

$$\psi(1.\omega.Fo) = 0 \tag{24-b}$$

$$\psi(\xi.0.Fo) = 0 \tag{24-c}$$

$$\frac{\partial \psi(\xi.1.Fo)}{\partial \omega} = \begin{cases} 0 & \xi < \xi_1 \\ 1 & \xi_1 < \xi < \xi_2 \\ 0 & \xi > \xi_2 \end{cases} \tag{24-d}$$

And also initial conditions by replacing Eq. (9) in primary conditions Eq. (8) are rewritten as follow:

$$\psi(\xi.\omega.0) = -\phi(\xi.\omega) \tag{25-a}$$

$$\frac{\partial \psi}{\partial Fo}(\xi.\omega.0) = 0 \tag{25-b}$$

The answer for differential Eq. (23) using variables' separation method is considered as follows:

$$\psi(\xi.\omega.Fo) = X(\xi)Z(\omega)\tau(Fo) \tag{26}$$

With applying Eq. (28), Eq. (25) is obtained as follow:

$$\frac{1}{\tau}\frac{\partial \tau}{\partial Fo} + \frac{Ve_q^2}{\tau}\frac{\partial^2 \tau}{\partial Fo^2} - \frac{Ve_T^2}{\tau}\frac{\partial \tau}{\partial Fo}\left(\frac{1}{X}\left(M^2 \frac{\partial^2 X}{\partial \xi^2} + \frac{M^2}{\xi}\frac{\partial X}{\partial \xi}\right) + \frac{1}{Z}\left(\frac{\partial^2 Z}{\partial \omega^2}\right)\right) = \frac{1}{X}\left(M^2 \frac{\partial^2 X}{\partial \xi^2} + \frac{M^2}{\xi}\frac{\partial X}{\partial \xi}\right) +$$
$$\frac{1}{Z}\left(\frac{\partial^2 Z}{\partial \omega^2}\right) = \pm\gamma^2 \pm \lambda^2 = \pm\upsilon^2 \tag{27}$$

Eq. (27) is divided into three distinct equations in terms of the variables ξ, ω and Fo. The separated equation in the direction of ξ is equal to:

$$\frac{\partial^2 X}{\partial \xi^2} + \frac{1}{\xi}\frac{\partial X}{\partial \xi} + \frac{\gamma^2}{M^2}X = 0 \tag{28}$$

$$\frac{\partial X(0)}{\partial \xi} = 0 \tag{29-a}$$

$$X(1) = 0 \tag{29-b}$$

With applying boundary conditions, the Eq. (28) is obtained as follow:

$$X(\xi) = CJ_0\left(\frac{\gamma}{M}\xi\right) \tag{30}$$

The separated equation in the direction ω and its corresponding boundary conditions are observed as Eqs. (31) and (32):

$$\frac{\partial^2 Z}{\partial \omega^2} + \lambda^2 Z = 0 \tag{31}$$

$$Z(0) = 0 \tag{32}$$

The differential Eq. (31) is calculated with applying boundary conditions Eq. (32) as follows:

$$Z(\omega) = A\sin(\lambda_g \omega) \tag{33}$$

In the Eq. (30) and Eq. (33), $\frac{\gamma}{M}$ and λ are the answers of the equations $J_0\left(\frac{\gamma}{M}\right) = 0$ and $\cos(\lambda) = 0$, respectively.

The separated equation in terms of Fo, dimensionless time variable is shown in Eq. (34):

$$Ve_q^2 \frac{\partial^2 \tau}{\partial Fo^2} + \left(1 + Ve_T^2 v^2\right)\frac{\partial \tau}{\partial Fo} + v^2 \tau = 0 \tag{34}$$

The initial condition is equal to:

$$\frac{\partial \tau}{\partial Fo}(0) = 0 \tag{35}$$

The answer of Eq. (34) is based on the existing conditions and divided into two parts of the complex and real answer.

If $\left(1 + Ve_T^2 v^2\right)^2 - 4v^2 Ve_q^2 > 0$, Eq. (34) has the following real answer:

$$\tau_{f.g}(t) = e^{-\frac{\left(1+Ve_T^2 v^2\right)Fo}{2Ve_q^2}}\left(C_1 \sinh\left(A_{fg}\frac{Fo}{2Ve_q^2}\right) + C_2 \cosh\left(A_{fg}\frac{Fo}{2Ve_q^2}\right)\right) \tag{36}$$

If $\left(1 + Ve_T^2 v^2\right)^2 - 4v^2 Ve_q^2 < 0$, Eq. (34) has an imaginary answer as follows:

$$\tau_{f.g}(t) = e^{-\frac{\left(1+Ve_T^2 v^2\right)Fo}{2Ve_q^2}}\left(C_1 \sin\left((A_{fg})_i \frac{Fo}{2Ve_q^2}\right) + C_2 \cos((A_{fg})_i \frac{Fo}{2Ve_q^2})\right) \tag{37}$$

C_1 and C_2 are constant coefficients of the equation obtained from the initial condition of Eq. (35). The value of A_{fg} is equal to:

$$A_{fg} = \sqrt{\left(1 + Ve_T^2 v^2\right)^2 - 4Ve_q^2 v^2}; \quad A_{fg} = i\left(A_{fg}\right)_i \tag{38}$$

The general solution of Eq. (34) is:

$$\tau_{f.g}(t) = C \begin{cases} e^{-\frac{\left(1+Ve_T^2 v^2\right)Fo}{2Ve_q^2}}\left[\frac{\left(1+Ve_T^2 v^2\right)}{A_{fg}}\sinh\left(A_{fg}\frac{Fo}{2Ve_q^2}\right) + \cosh\left(A_{fg}\frac{Fo}{2Ve_q^2}\right)\right] \\ e^{-\frac{\left(1+Ve_T^2 v^2\right)\xi}{2Ve_q^2}}\left[\frac{\left(1+Ve_T^2 v^2\right)}{(A_{fg})_i}\sin\left((A_{fg})_i \frac{Fo}{2Ve_q^2}\right) + \cos\left((A_{fg})_i \frac{Fo}{2Ve_q^2}\right)\right] \end{cases} \tag{39}$$

The general solution of Eq. (23) is obtained by replacing the solutions of Eq. (30), Eq. (33) and Eq. (39) in Eq. (26) as follows:

$$\psi(\eta.\omega.\xi) = \sum_{f=1}^{F}\sum_{g=0}^{G} C_{fg}\, e^{-\frac{(1+Ve_T^2 v^2)Fo}{2Ve_q^2}}\left[\frac{(1+Ve_T^2 v^2)}{A_{fg}}\sinh\left(A_{fg}\,\frac{Fo}{2Ve_q^2}\right)+\right.$$

$$\cosh\left(A_{fg}\,\frac{Fo}{2Ve_q^2}\right)\right]\times \sin(\lambda\omega)J_0\left(\frac{\gamma_f}{M}\xi\right)+\sum_{f=F+1}^{\infty}\sum_{g=G+1}^{\infty} C_{fg}\, e^{-\frac{(1+Ve_T^2 v^2)\xi}{2Ve_q^2}}\times$$

$$\left[\frac{(1+Ve_T^2 v^2)}{(A_{fg})_i}\sin\left((A_{fg})_i\,\frac{Fo}{2Ve_q^2}\right)+\cos\left((A_{fg})_i\,\frac{Fo}{2Ve_q^2}\right)\right]\times \sin(\lambda\omega)J_0\left(\frac{\gamma_f}{M}\xi\right) \tag{40}$$

Using the initial condition Eq. (25-a) and the orthogonal function, C_{fg} is equal to

$$C_{fg} = -2\, a_f\, \gamma_f\, \cosh(\gamma_f)\frac{(-1)^g}{(\gamma_f^2+\lambda_g^2)} \tag{41}$$

$$C_{fg} = \frac{-4M\left(-\xi_1 J_1\left(\frac{\gamma_f}{M}\xi_1\right)+\xi_2 J_1\left(\frac{\gamma_f}{M}\xi_2\right)\right)}{\gamma_f\left[J_1\left(\frac{\gamma_f}{M}\right)\right]^2}\frac{(-1)^g}{(\gamma_f^2+\lambda_g^2)} \tag{42}$$

4 Results and discussion

In this section, first results of this investigation are compared with results of Saedodin et al. [Saedodin and Barforoush (2012, 2017)]. After that in second section results of 2D non-Fourier heat conduction are presented. For verification this work, $\tau_T = 0$, $\xi_2 = 1$ and Saedodin's problem's boundary conditions are applied; comparing results of current work and Barforoush are shown in Figs. 2-4. According to the results, there are no differences between two works and this work is absolutely compatible with Saedodin's work.

Fig. 2 shows changing of dimensionless temperature across radius direction in the different Vernotte numbers. In the C-V hyperbolic heat conduction, increasing relaxation time causes decreasing thermal wave speed, so thermal wave needs more time to sense another side of cylinder.
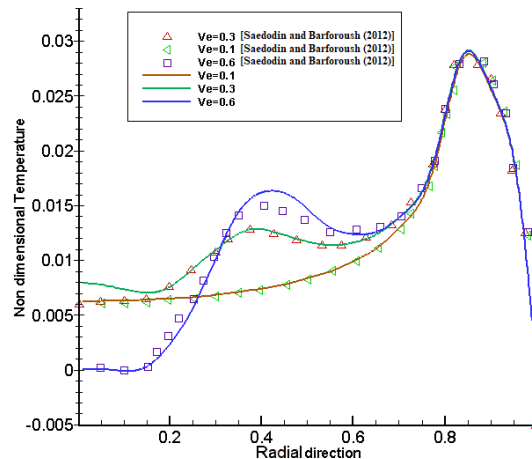
Figure 2: Comparison of Saedodin's work [Saedodin and Barforoush (2012)] with current work ($\xi_1 = 0.8. \xi_2 = 1\ Fo = 0.1.\ Ve_T = 0\ \xi_2 = 1. M = 16$)

Comparison of three dimensional temperature gradient in Saedodin and Barforoush's et al. work with current work is shown in Figs. 3-4. Behavior of thermal waves is the same in the both works. Fig. 3 is shown for $Ve_q = 0.3$ and another one (Fig. 4) is shown for $Ve_q = 0.6$ so by increasing of relaxation time, heat transfer behaves more wavy.
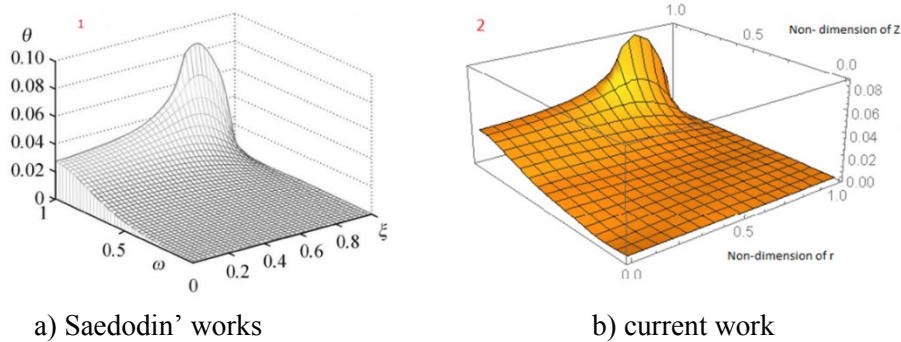

a) Saedodin' works   b) current work

Figure 3: Comparison of three dimensional temperature gradient in Saedodin and Barforoush's work with this work
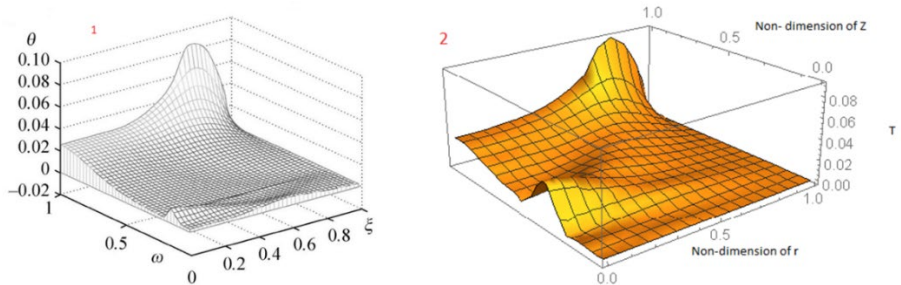($Fo = 0.5. M = 4; Ve_q = 0.3\ Ve_T = 0. \xi_1 = 0.7. \xi_2 = 1$)

Figure 4: Comparison of three dimensional temperature gradient in Saedodin and Barforoush's work with this work
($Fo = 0.5. M = 4; Ve_q = 0.6\ Ve_T = 0 . \xi_1 = 0.7\ \xi_2 = 1$)

In order to simulate and plot the charts, the values $\xi_1 = 0.4$ and $\xi_2 = 0.6$ have been assumed and investigated.

Fig. 5 shows the analytical answer of the problem in three states of heat transfer with Fourier equations, single phase lag and dual phase lag in the cylinder axis in terms of dimensionless time. It can be seen that in single and dual phase lags, in contrast to Fourier state, there is a time lag of 0.1 to 0.2 s. This time lag indicates the limitation of the heat wave rate and the time it takes to transfer the effect of applying heat flux across the cylinder axis. Also, the single-phase lag model exhibits more wave-like properties than dual phase and Fourier models. This model not only has more time lag at the beginning, but also needs more time to reach the stable temperature.
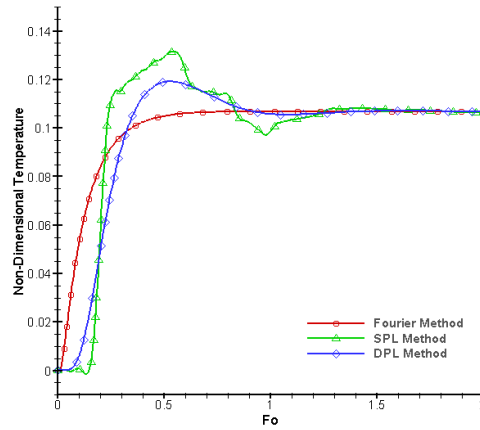
Figure 5: Dimensionless temperature change diagram to dimensionless time in three states of Fourier, single phase lag and dual phase lag ($\xi = 0.\omega = 1.M = 1$)

Fig. 6 shows changes in dimensionless temperature across the cylinder axis for heat transfer with Fourier, single phase lag, and dual phase lag equations. It is observed that the maximum temperature has occurred in the single phase lag model. The reason for this is that the single-phase lag model did not reach a stable temperature of 0.2. It is also observed in this figure that the rate of propagation of heat wave in Fourier and dual phase lag methods is higher than the single-phase lag method.
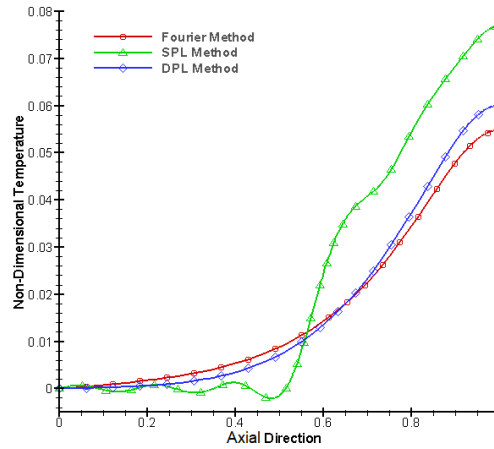

Figure 6: Changes in dimensionless temperature across the cylinder ($\xi = 0.Fo = 0.2.M = 2.Ve_T = 0.2.Ve_q = 0.5$)

Fig. 7 shows changes in dimensionless temperature along the radius of the cylinder for heat transfer with Fourier equations, single phase lag, and dual phase lag. The maximum temperature changes occurred at the site of the application of constant heat flux.
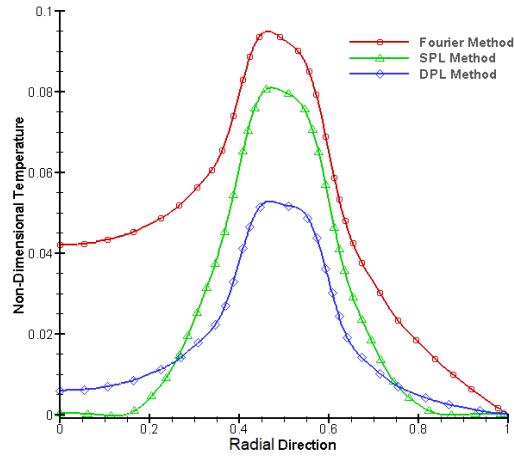
Figure 7: Temperature change diagrams along the radius of the cylinder (ω = 1 Fo = 0.05.M = 2,$\boldsymbol{Ve_T = 0.2.Ve_q = 0.5}$)

Fig. 8 shows isothermal lines along ξ and ω based on dual phase lag model. In this figure, isothermal lines' density at the site of constant heat flux boundary is clearly visible. Due to the boundary condition θ (1, ω, Fo)=0, heat flux moves along the radius toward the center of the cylinder.
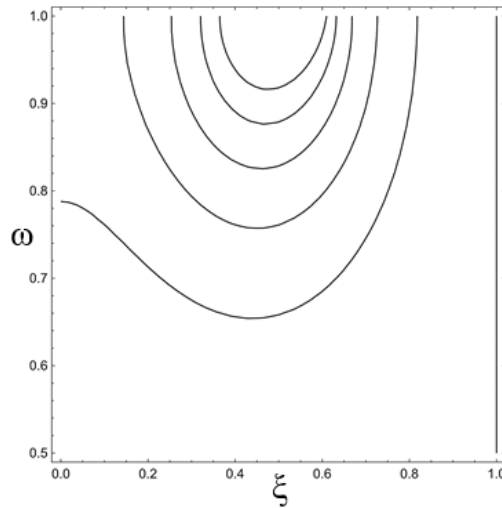

Figure 8: Isothermal lines along ξ and ω based on dual phase lag model $\left(\boldsymbol{Fo = 0.2.M = 1.Ve_T = 0.2.Ve_q = 0.5}\right)$

The response of the analysis of dimensionless temperature at dimensionless time for dual phase lag model in terms of various ratios of length to the radius of the cylinder (M) can be seen in Fig. 9. According to Fig. 9, the longer the ratio of the length to the radius of the cylinder (M), the less time for the temperature to reach a steady state. Also, with increasing

the ratio of length to radius of the cylinder, primary time lag also reduced. For example, at M=1, primary time lag is approximately 0.1, which is reduced to 0.05 at M=2.
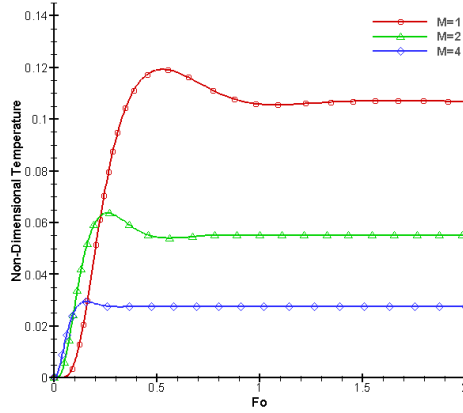

Figure 9: Changes in dimensionless temperature and dimensionless time at different ratios of cylinder length-radius $\left(Fo = 0.2. Ve_T = 0.2. Ve_q = 0.5\right)$

Fig. 10 shows changes in the increase of heat flux phase lag on dimensionless temperature in the dual phase lag model in the range of 0 to 4. In this figure, it can be seen that with constant temperature gradient time lag and increased heat flux, the wave properties increase and the amount of time lag initially increases and the system also needs more time to reach the steady-state temperature.
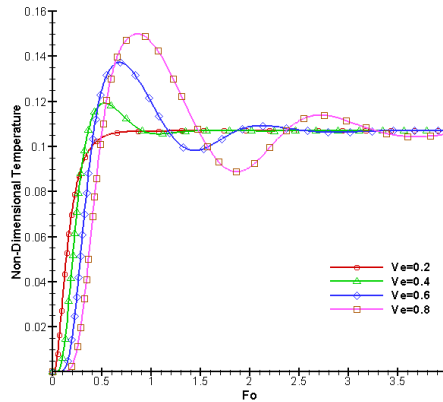

Figure 10: The effect of lag of different times of heat flux on dimensionless temperature ($\xi = 0.\omega = 1 . M = 1. Ve_T = 0.2.$)

Fig. 11 shows the effect of time lag changes in the temperature gradient on the dimensionless temperature profile. As shown in Fig. 11, in a low temperature gradient lag, the amount of heat wave propagation is very small and mild, which heat wave propagation increases with increasing the time lag of the temperature gradient. Meanwhile, with fixing

time lag of heat flux and increasing temperature gradient time lag, with the wave sentence in dual phase lag model, non-wave behavior for heat transfer is predicted, and dual phase lag model is similar to Fourier state.
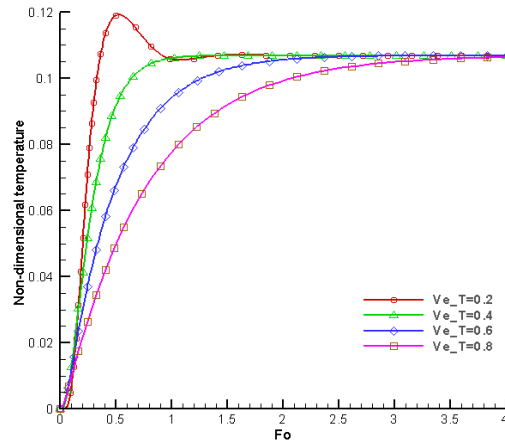

Figure 11: The effect of different times' lag of temperature gradient on dimensionless temperature

5 Conclusion

In this study, the exact solution of the non-Fourier heat transfer equation was obtained based on the dual phase lag in a solid cylinder by applying constant axial heat flux and compared with the results of Fourier heat transfer equation and the fuzzy change. According to the results, the single phase lag model exhibits more wave properties than the dual phase lag model. This feature requires more time to achieve a steady state. Meanwhile, the propagation rate of the heat wave in the dual phase lag model is greater than the single phase lag, although the maximum temperature occurs in the single phase lag model. With increasing time lag of heat flux and temperature gradient time lag the time to reach the stable temperature increased, with the difference that the increase in the time lag of heat flux increases the wave properties, but, in contrast the increase in temperature gradient time lag will neutralize the wave properties and increases heat release. Also, increasing the length to radius ratio reduces the time to reach the stable temperature in the dual phase lag model.

Conflicts of Interest: We declare that we have no financial or personal relationships with other people or organizations that could inappropriately influence (bias) our work entitled "Numerical Analysis of Non-Fourier Heat Transfer in a Solid Cylinder with Dual-Phase-Lag Phenomenon".

References

Abdel-Hamid, B. (1999): Modelling non-Fourier heat conduction with periodic thermal oscillation using the finite integral transform. *Applied Mathematical Modelling*, vol. 23, no. 12, pp. 899-914.

Delouei, A. A.; Norouzi, M. (2015): Exact analytical solution for unsteady heat conduction

in fiber-reinforced spherical composites under the general boundary conditions. *Journal of Heat Transfer*, vol. 137, no. 10, pp. 1-8.

Anbarloei, M.; Shivanian, E. (2016): Exact closed-form solution of the nonlinear fin problem with temperature-dependent thermal conductivity and heat transfer coefficient. *Journal of Heat Transfer*, vol. 138, no. 11, pp. 1-6.

Antaki, P. J. (2005): New interpretation of non-Fourier heat conduction in processed meat. *Journal of Heat Transfer*, vol. 127, no. 2, pp. 189-193.

Askarizadeh, A.; Baniasadi, E. (2017): Equilibrium and non-equilibrium thermodynamic analysis of high-order dual-phase-lag heat conduction. *International Journal of Heat and Mass Transfer*, vol. 104, pp. 301-309.

Askarizadeh, H.; Ahmadikia, H. (2018): Extended irreversible thermodynamics *vs.* second law analysis of high-order dual-phase-lag heat transfer. *Journal of Heat Transfer*, vol. 140, no. 8, pp. 1-9.

Babaei, M. H.; Chen, Z. T. (2008): Hyperbolic heat conduction in a functionally graded hollow sphere. *International Journal of Thermophysics*, vol. 29, no. 4, pp. 1457-1469.

Bahrami, A.; Hosseinzadeh, S.; Ghasemiasl, R.; Radmanesh, M. (2015): Solution of non-Fourier temperature field in a hollow sphere under harmonic boundary condition. *Applied Mechanics and Materials*, vol. 772, pp. 197-203.

Cattaneo, C. (1958): A form of heat conduction equation which eliminates the paradox of instantaneous propagation. *Compte Rendus*, vol. 247, pp. 431-433.

Cimmelli, V.; Frischmuth, K. (1996): Hyperbolic heat conduction at cryogenic temperatures. *Reniconti Del Circolo Matematico Di Palermo*, vol. 45, pp. 137-145.

Fu, J. W.; Chen, Z. T.; Qian, L. F.; Hu, K. Q. (2014): Transient thermoelastic analysis of a solid cylinder containing a circumferential crack using the c-v heat conduction model. *Journal of Thermal Stresses*, vol. 37, no. 11, pp.1324-1345.

Jiang, F. M. (2006): Solution and analysis of hyperbolic heat propagation in hollow spherical objects. *Heat and Mass Transfer*, vol. 42, pp. 1083-1091.

Julius, S.; Leizeronok, B.; Cukurel, B. (2018): Nonhomogeneous dual-phase-lag heat conduction problem: analytical solution and select case studies. *Journal of Heat Transfer*, vol. 140, no. 3, pp. 31301-31322.

Liu, K. C.; Chang, P. C. (2007): Analysis of dual-phase-lag heat conduction in cylindrical system with a hybrid method. *Applied Mathematical Modelling*, vol. 31, no. 2, pp. 369-380.

Maurer, M.; Thompson, H. A. (1973): Non-Fourier effects at high heat flux. *Journal of Heat Transfer*, vol. 95, no. 2, pp. 284-286.

Moosaie, A. (2008): Axisymmetric non-Fourier temperature field in a hollow sphere. *Archive of Applied Mechanics*, vol. 75, pp. 679-694.

Moosaie, A.; Atefi, G.; Fardad, A. (2008): Two-dimensional non-Fourier heat conduction with arbitrary initial and periodic boundary conditions. *Forsch Ingenieurwes*, vol. 72, pp. 67-76.

Özisik, M. N.; David, W. H. (2013): *Heat Conduction*, 3rd Edition New Jersey: Wiley.

Qiu, T. Q.; Tien, C. L. (1993): Heat transfer mechanisms during short-pulse laser heating

of metals. *Journal of Heat Transfer*, vol. 115, no. 4, pp. 835-841.

Saedodin, S.; Barforoush, M. S. M. (2012): An exact solution for thermal analysis of a cylindrical object using a hyperbolic heat conduction model. *Heat Transfer Research*, vol. 43, no. 5, pp. 405-423.

Saedodin, S.; Barforoush, M. S. M. (2017): An exact solution for thermal analysis of a cylindrical object using hyperbolic thermal conduction model. *Thermophysics and Aeromechanics*, vol. 24, no. 6, pp. 909-920.

Shirmohammadi, R. (2008): Temperature transients in spherical medium irradiated by laser pulse. *International Communications in Heat and Mass Transfer*, vol. 35, pp. 1017-1023.

Talaee, M. R.; Sarafrazi, V.; Bakhshandeh, S. (2016): Exact analytical hyperbolic temperature profile in a three-dimensional media under pulse surface heat flux. *Journal of Mechanics*, vol. 32, no. 3, pp. 339-347.

Talaee, M. R.; Atefi, G. (2011): Non-Fourier heat conduction in a finite hollow cylinder with periodic surface heat flux. *Archive of Applied Mechanics*, vol. 81, no. 12, pp. 1793-1806.

Tang, D. W.; Araki, N. (1999): Wavy, wavelike, diffusive thermal responses of finite rigid slabs to high-speed heating of laser-pulses. *International Journal of Heat and Mass Transfer*, vol. 42, no. 5, pp. 855-860.

Tsai, C. S.; Lin, Y. C.; Hung, C. I. (2005): A study on the non-Fourier effects in spherical media due to sudden temperature changes on the surface. *Heat and Mass Transfer*, vol. 41, pp. 709-716.

Tsai, C.; Hung, C. (2003): Thermal wave propagation in bi-layered composite sphere due to sudden temperature change on the outer surface. *International Journal of Heat and Mass Transfer*, vol. 46, pp. 5137-5144.

Tzou, D. Y. (1992): Thermal shock phenomena under high-rate response in solids. *Annual Review of Heat Transfer*, vol. 4, pp. 111-185.

Tzou, D. Y. (1995): A unified field approach for heat conduction from micro- to macro-scales. *Journal of Heat Transfer*, vol. 117, no. 1, pp. 8-16.

Tzou, D. Y. (2014): *Macro-to Microscale Heat Transfer: The Lagging Behavior*, 2nd Edition, Wiley.

Vernotee, P. (1958): Les paradoxes de la theorie continue de 1 equationdel la Chaleur. *Compte Rendus*, vol. 246, pp. 3154-3155.

Wang, L.; Zhou, X. S.; Wei, X. H. (2008): *Heat Conduction (Mathematical Models and Analytical Solutions)*. Department of Mechanical Engineering. University of Hong Kong.

Wang, L. Q.; Xu, M. T.; Zhou, X. S. (2001): Well-posedness and solution structure of dual-phase-lagging heat conduction. *International Journal of Heat and Mass Transfer*, vol. 44, pp. 1659-1669.

Wu, T. S.; Lee, H. L.; Chang, W. J.; Yang, Y. C. (2015): An inverse hyperbolic heat conduction problem in estimating pulse heat flux with a Dual-Phase-Lag model. *International Communications in Heat and Mass Transfer*, vol. 60, pp. 1-8.

Xu, M. T. (2011): Thermodynamic basis of Dual-Phase-Lagging heat conduction. *Journal of Heat Transfe*, vol. 133, no. 4, pp. 1-7.